Mathematical Biosciences and Engineering

http://www.aimspress.com/journal/mbe

MBE, 21(4): 5826–5837.
DOI: 10.3934/mbe.2024257
Received: 11 December 2023
Revised: 05 February 2024
Accepted: 20 February 2024
Published: 28 April 2024

Research article

Bayesian inverse problem for a fractional diffusion model of cell migration

Francisco Julian Ariza-Hernandez[1], Juan Carlos Najera-Tinoco[1], Martin Patricio Arciga-Alejandre[1], Eduardo Castañeda-Saucedo[2] and Jorge Sanchez-Ortiz[1,*]

[1] Faculty of Mathematics, Autonomous University of Guerrero, Mexico

[2] Laboratory of Cancer Cell Biology, Faculty of Chemical and Biological Sciences, Autonomous University of Guerrero, Mexico

* **Correspondence:** Email: jsanchez@uagro.mx.

Abstract: In the present work, both direct and inverse problems are considered for a Fisher-type fractional diffusion equation, which is proposed to describe the phenomenon of cell migration. For the direct problem, a solution is given via the Fourier method and the Laplace transform. On the other hand, we solved the inverse problem from a Bayesian statistical framework using a set of data that are the result of a cell migration experiment on a wound closure assay. We estimated the parameters of the mathematical model via Markov Chain Monte Carlo methods.

Keywords: cell migration; fractional derivative; Bayesian estimation

1. Introduction

Cell migration plays important roles in many biological processes that require the generation and regeneration of tissues, and is involved in processes such as morphogenesis, embryonic development, and wound healing [1, 2]. Similarly, cell migration is responsible for pathological processes such as the invasion of tumor cells into adjacent tissues, the formation of new blood vessels in tumors, and the metastasis of tumor cells to distant regions in the body [3–5]. The in vitro cell migration assay is a very important method to study this phenomenon. The procedure involves incubation of cells until they completely cover the bottom of the cultivation plate forming a monolayer and the creation of an artificial wound (on the monolayer). After injury, the cells rapidly migrate to the vicinity of the wound to close it; over time, the cells will fill the wound. It has been observed that cell motility decreases with increasing local density [6–8]. In 1990, Sherrat and Murray [9] considered a model consisting of a conservation equation for cell density per unit area, where he used the term diffusion to model cell migration by relying on the Fisher equation. Similarly, in 2004, Maini et al. [10] developed a model to quantify mesothelial cell migration, interpreting the results using the Fisher equation, relating the

diffusion coefficient and the cell proliferation rate. Subsequently, in 2015, Stonko et al. [11] studied cell migration by implementing a model using identical mathematical cells (IMCs), where specific biophysical properties are assigned to each IMC in order to mimic a diversity of cells.

The latest advances on cell migration have been in continuous nonlocal models, mainly from the perspective of its involvement in embryonic development and cancer invasion and its development. In 2020, Chen et al. [12] described a systematic classification of models in partial differential equations (PDEs) that fall into the reaction-diffusion-advection (RDA) class.

The dynamics of certain phenomena are subject to drastic changes in magnitude, for example, diffusive ones, which implies that these are anomalous. Such dynamics often cannot be modeled with integer linear differential equations since they follow certain non-locality rules, which is precisely why the fractional derivative plays a decisive role in modeling anomalous dynamics. This can be seen as an alternative to nonlinear models, and provides a better fit compared to ordinary models for the description of the phenomena [13, 14]. On the other hand, the fractional derivative has an associated memory index of the system, which implies that the information of the fractional derivative at a fixed time is determined by its previous states. This property is important in biological systems because the governing evolution laws have this characteristic [15]. In this work, we use a Fisher-type fractional diffusion equation

$$D_t^{\alpha} u(x,t) = a u_{xx}(x,t) + b u(x,t), \tag{1.1}$$

where $u(x,t)$ represents the cell density at position x and time t, the constant parameter a is known as the diffusion coefficient, b represents the rate of cell density growth, and D_t^{α} is the Caputo fractional derivative.

2. Materials and methods for the wound closure assay

The HaCaT cell line (ATCC, Manassas, VA, USA) was cultivated in 10% DMEM/F12 (D8900, Sigma- Aldrich) supplemented with 10% fetal bovine serum SFB (By Productos, Guadalajara, Jal, Mexico) and antibiotic-antimycotic (15240, Gib-co) at 37 °C in a humidified atmosphere containing 5% CO_2. HaCaT cells were cultured in 60 mm cultivation plates until they reached 100% confluence. Once confluence was reached, the cells were cultivated in a DMEM/F12 environment without SFB for 12 h, plus a 2 h treatment with 10 μM AraC to inhibit cell proliferation. After pretreatment with the proliferation inhibitor, the cell monolayer was scratched using a 200 μL sterile pipette tip, washed twice with 1 mL of PBS 1X to remove the detached cells, and mantained in DMEM/F12 supplemented with 2% SFB. The cells were incubated for 24 h at 37°C in a 5% CO_2 atmosphere. Phase contrast images were acquired at the same wound site every 6 h through an EVOs FL automated microscope (Life Technologies Corporation; Carlsbad, CA, USA) using a 10x objective. Cell counting was performed using the Image J software.

The wound closure assay is based on the observation over time of the change produced in a monolayer of cells that have been wounded. Basically, the procedure consists of four phases (See Figure 1):

1) Cells are cultivated on a 2D surface until they form a confluent monolayer.

2) A physical gap is created within a cell monolayer.

3) The monolayer responds with cell movement to the empty region until the wound is closed.

4) The process of cell migration from the cells at the edge of the gap to the center of the wound is monitored. Microscopy images are captured at different time lapses during the assay.

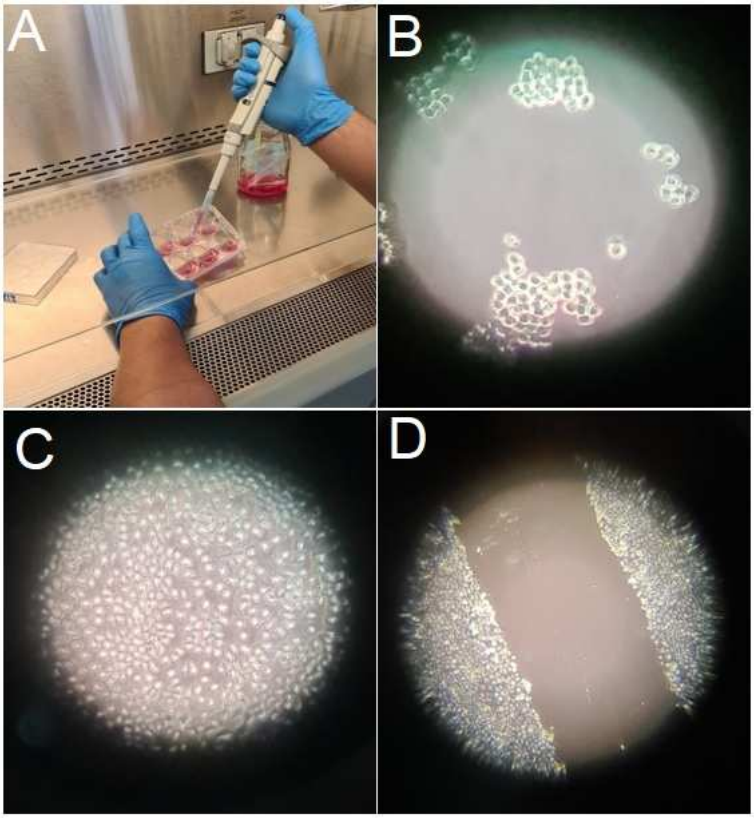

Figure 1. A) Generation of the artificial wound in the cell monolayer. B) Representative image of HaCaT cells at low confluence. C) Representative image of a confluent HaCaT cell monolayer. D) Representative image of the a wound generated on the confluent monolayer.

3. Fractional heat equation

In this section, we are going to describe the change of the cell density $u(x,t)$ during the wound closure assay through a mathematical model, which consists of a Neumann initial-boundary value problem for a diffusion-reaction equation with fractional time derivative

$$\begin{cases} D_t^\alpha u(x,t) = a u_{xx}(x,t) + b u(x,t), & t > 0, \alpha \in (0,1], \\ u_x(0,t) = u_x(L,t) = 0, & 0 < x < L, t > 0, \\ u(x,0) = g(x), & 0 < x < L, \end{cases} \tag{3.1}$$

where the Caputo fractional derivative is defined as

$$D_t^\alpha u(x,t) = \frac{1}{\Gamma(1-\alpha)} \int_0^t \frac{u_\tau(x,\tau)}{(t-\tau)^\alpha} d\tau, \quad \alpha \in (0,1],$$

where Γ is the Gamma function and u_τ is the ordinary partial derivative of u with respect to time. Although model (3.1) is not bounded with respect to time, it is proposed in this way since the cell migration experiment is carried out in a short time.

We keep the boundary values for the derivative of the solution equal to zero, $u_x(0,t) = u_x(L,t) = 0$, since there is no flow of cells across the boundary of the petri dish. Likewise, knowing the structure of the cells at time $t = 0$, we obtain the initial condition for the model $u(x,0) = g(x), 0 < x < L$.

For the first equation in model (3.1), we use the method of separation of variables. We suppose that

$$u(x,t) = X(x)T(t).$$

Then, substituting the above equation in model (3.1), we get the following system of ordinary differential equations:

$$X''(x) - kX(x) = 0, \tag{3.2}$$

$$D_t^\alpha T(t) - (b + ak)T(t) = 0, \tag{3.3}$$

where k is a constant. When solving Eq (3.2), taking into account the boundary conditions, we obtain the following solutions:

$$X_n(x) = A_n \cos\left(\sqrt{-k}x\right), \quad k = -\left(\frac{n\pi}{L}\right)^2, \quad n = 0, 1, 2, \ldots, \tag{3.4}$$

where A_n are arbitrary constants. Using the Laplace transform defined by

$$\mathscr{L}\{T(t)\}(s) = \int_0^\infty e^{-st}T(t)dt, \qquad \Re e(s) > \gamma,$$

where $T(t)$ is a real-valued function of exponential order γ, and its inverse is defined as

$$T(t) = \frac{1}{2\pi i}\int_{\gamma-i\infty}^{\gamma+i\infty} e^{st}\mathscr{L}\{T(t)\}(s)\,ds, \tag{3.5}$$

since γ is to the right of all singularities of the function T. Thus, in Eq (3.3), we get

$$\mathscr{L}\{T_n(t)\}(s) = \frac{B_n s^{\alpha-1}}{s^\alpha - (b + ak)},$$

where $T_n(0) = B_n$, and

$$T_n(t) = B_n\mathscr{L}^{-1}\left\{\frac{s^{\alpha-1}}{s^\alpha - (b + ak)}\right\} = B_n E_\alpha\left[(b + ak)t^\alpha\right], \tag{3.6}$$

where E_α is the Mittag-Leffler function defined as follows:

$$E_\alpha(z) = \sum_{k=0}^{\infty}\frac{z^k}{\Gamma(\alpha k + 1)}, \quad z \neq 0,$$

where $E_\alpha(0) = 1$, for $\alpha > 0$. Then, by Eqs (3.4) and (3.6), $u_n(x,t) = X_n(x)T_n(t)$ is a solution of model (3.1) for each n. Finally, by linearity, the general solution is given by

$$u(x,t) = \sum_{n=0}^{\infty} C_n \cos\left(\frac{n\pi}{L}x\right) E_\alpha\left[\left(b - a\left(\frac{n\pi}{L}\right)^2\right)t^\alpha\right], \tag{3.7}$$

where $C_n = A_n B_n$. Now, using the initial condition, we get a cosine Fourier series

$$g(x) = u(x,0) = \sum_{n=0}^{\infty} C_n \cos\left(\frac{n\pi}{L}x\right), \quad 0 < x < L.$$

where

$$C_n = \frac{2}{L}\int_0^L g(x)\cos\left(\frac{n\pi}{L}x\right)dx,$$

by orthogonality of $\left\{\cos\left(\frac{n\pi}{L}x\right)\right\}$.

4. Bayesian statistical inversion

Note that for model (3.1) we have the following observation equation:

$$y_{ij} = u(x_i, t_j|\boldsymbol{\omega}) + \epsilon_{ij}, \;\; i = 0, 1, 2, ..., m, \;\; j = 1, 2, ..., T, \tag{4.1}$$

where $u(x_i, t_j|\boldsymbol{\omega})$ is obtained from Eq (3.7) for a fixed parameter vector $\boldsymbol{\omega} = (a, b, \alpha)'$, and y_{ij} corresponds to the cell density obtained from the wound closure assay in the section (space) i at time j, so we can form a matrix of observations

$$\mathbf{Y} = \begin{pmatrix} y_{11} & y_{12} & \cdots & y_{1T} \\ y_{21} & y_{22} & \cdots & y_{2T} \\ \vdots & \vdots & \ddots & \vdots \\ y_{m1} & y_{m2} & \cdots & y_{mT} \end{pmatrix}$$

where ϵ_{ij} are the measurement errors, which are considered to be independent random variables identically distributed (iid) of a normal distribution; that is,

$$\epsilon_{ij} \sim \mathcal{N}\left(0, \sigma^2\right).$$

Consequently, the observations y_{ij} are now random variables with normal probability density function with mean $u(x_i, t_j|\boldsymbol{\omega})$ and variance σ^2, which is given by

$$f(y_{ij}|\boldsymbol{\theta}) = \frac{1}{\sqrt{2\pi}\sigma} exp\left\{-\frac{1}{2\sigma^2}\left[y_{i,j} - u(x_i, t_j|\boldsymbol{\omega})\right]^2\right\}, \;\; -\infty < y_{ij} < \infty,$$

where $\boldsymbol{\theta} = (a, b, \alpha, \sigma^2)'$ contain all the parameters of interest. Then, we obtain the likelihood function

$$L(\mathbf{Y}|\boldsymbol{\theta}) = \prod_{i=1}^{m}\prod_{j=1}^{T} f(y_{i,j}|\boldsymbol{\theta}) = (2\pi\sigma)^{-mT} exp\left\{-\frac{1}{2\sigma^2}\sum_{i=1}^{m}\sum_{j=1}^{T}\left[y_{i,j} - u(x_i, t_j|\boldsymbol{\omega})\right]^2\right\}. \tag{4.2}$$

We define prior distributions for $\boldsymbol{\theta}$ according to prior-knowledge as follows:

$$\begin{aligned} a &\sim Gamma(\alpha_a, \beta_a), \quad 0 < a < \infty, \ \ \alpha_a > 0, \ \ \beta_a > 0, \\ b &\sim Normal(\alpha_b, \beta_b), \quad -\infty < b < \infty, \\ \alpha &\sim Beta(\tau_\alpha, \beta_\alpha), \quad 0 < \alpha < 1, \ \ \tau_\alpha > 0, \ \ \beta_\alpha > 0, \\ \sigma^2 &\sim IGamma(\alpha_{\sigma^2}, \beta_{\sigma^2}). \end{aligned}$$

The parameters involved in the prior distributions are called hyperparameters. Assuming prior independence of the parameters, we can write the joint prior distribution as

$$p(\boldsymbol{\theta}|hyperparameters) \propto p(a|\alpha_a, \beta_a)p(b|\alpha_b, \beta_b)p(\alpha|\tau_\alpha, \beta_\alpha)p(\sigma^2|\alpha_{\sigma^2}, \beta_{\sigma^2}). \tag{4.3}$$

Substituting each distribution, we have

$$\begin{aligned} p(\boldsymbol{\theta}|\text{hyperparameters}) \quad = \quad & \frac{1}{\Gamma(\alpha_a)\beta_a^{\alpha_a}} a^{\alpha_a - 1} \exp\left\{\frac{-a}{\beta_a}\right\} \frac{1}{\sqrt{2\pi}\beta_b} \exp\left\{-\frac{1}{2\beta_b^2}(b - \alpha_b)^2\right\} \\ & \times \frac{1}{B(\tau_\alpha, \tau_\alpha)} \alpha^{\tau_\alpha - 1}(1 - \alpha)^{\beta_\alpha - 1} \frac{\beta_{\sigma^2}^{\alpha_{\sigma^2}}}{\Gamma(\alpha_{\sigma^2})} \left(\frac{1}{\sigma^2}\right)^{\alpha_{\sigma^2}+1} \exp\left\{\frac{-\beta_{\sigma^2}}{\sigma^2}\right\}. \end{aligned} \tag{4.4}$$

In this way, using Bayes' Theorem we can identify the posterior distribution, which is given by

$$p(\boldsymbol{\theta}|\mathbf{Y}) = \frac{L(\mathbf{Y}|\boldsymbol{\theta})p(\boldsymbol{\theta})}{\int_\Theta L(\mathbf{Y}|\boldsymbol{\theta})p(\boldsymbol{\theta})d\boldsymbol{\theta}},$$

where Θ denotes the parametric space of $\boldsymbol{\theta}$. Since the denominator in the rigth hand side of the above equation does not depend of $\boldsymbol{\theta}$, then the posterior distribution can be obtained from the proportional relation:

$$\begin{aligned} p(\boldsymbol{\theta}|\mathbf{Y}) \propto & (2\pi\sigma)^{-mT} \exp\left\{-\frac{1}{2\sigma^2}\sum_{i=1}^{m}\sum_{j=1}^{T}\left[y_{i,j} - \sum_{n=0}^{\infty} C_n \cos\left(\frac{n\pi}{L}x_i\right) E_\alpha\left[\left(b - a\left(\frac{n\pi}{L}\right)^2\right)t_j^\alpha\right]\right]^2\right\} \\ & \times \frac{1}{\Gamma(\alpha_a)\beta_a^{\alpha_a}} a^{\alpha_a - 1} \exp\left\{\frac{-a}{\beta_a}\right\} \frac{1}{\sqrt{2\pi}\beta_b} \exp\left\{-\frac{1}{2\beta_b^2}(b - \alpha_b)^2\right\} \\ & \times \frac{1}{B(\tau_\alpha, \tau_\alpha)} \alpha^{\tau_\alpha - 1}(1 - \alpha)^{\beta_\alpha - 1} \frac{\beta_{\sigma^2}^{\alpha_{\sigma^2}}}{\Gamma(\alpha_{\sigma^2})} \left(\frac{1}{\sigma^2}\right)^{\alpha_{\sigma^2}+1} \exp\left\{\frac{-\beta_{\sigma^2}}{\sigma^2}\right\}. \end{aligned} \tag{4.5}$$

The above posterior distribution does not have a known analytical form, and so we use Markov Chain Monte Carlo (MCMC) techniques to obtain samples of the marginal posterior distributions of the parameters. Some of the most widely used methods are Gibbs sampling, which is flexible to adapt to different changes, and it allows us to calculate numerical estimates of marginal probability distributions [16]. The Metropolis-Hastings algorithm is a powerful Markov chain method for simulating multivariate distributions [17], among others. Currently, the vast majority of MCMC algorithms have been implemented in software, such as WinBUGS and JAGS, and all of these software packages provide programs for Bayesian modeling through posterior simulation given a

model and specific data. Within the R statistical software [18] packages such as R2WinBUGS [19], R2jags [20] and rjags [21], allow for running WinBUGS and JAGS from within the R software. In this work, we use the JAGS package inside R to determine samples of the a posteriori distribution of each of the parameters of interest; RealSlicer is a JAGS-specific sampler that uses slice sampling to effectively and adaptively sample continuous variables [22].

5. Data and results

In this section, the data obtained from the wound clousure assay experiment in the laboratory are presented (see Figure 2). Once the cell migration assay was performed, a set of data was obtained by calculating the cell density along the wound. Each image was divided into 49 vertical sections. The cell density in each section was calculated by counting the number of cells per section, and four sets were captured at different times, 0, 8, 16 and 24 hours, and the data are displayed in Figure 3.

The estimation was performed in two cases: (*i*) for alpha fixed equal to 1 and (*ii*) for alpha between (0,1). By means of the deviance information criterion (DIC), the model for the estimated alpha between (0,1) is preferred to the corresponding model with alpha equal to 1, since $\text{DIC}_{ii} = -129.6 < -114.9 = \text{DIC}_i$, where DIC_i and DIC_{ii} corresponds to estimated DIC for the cases (*i*) and (*ii*), described above, respectively.

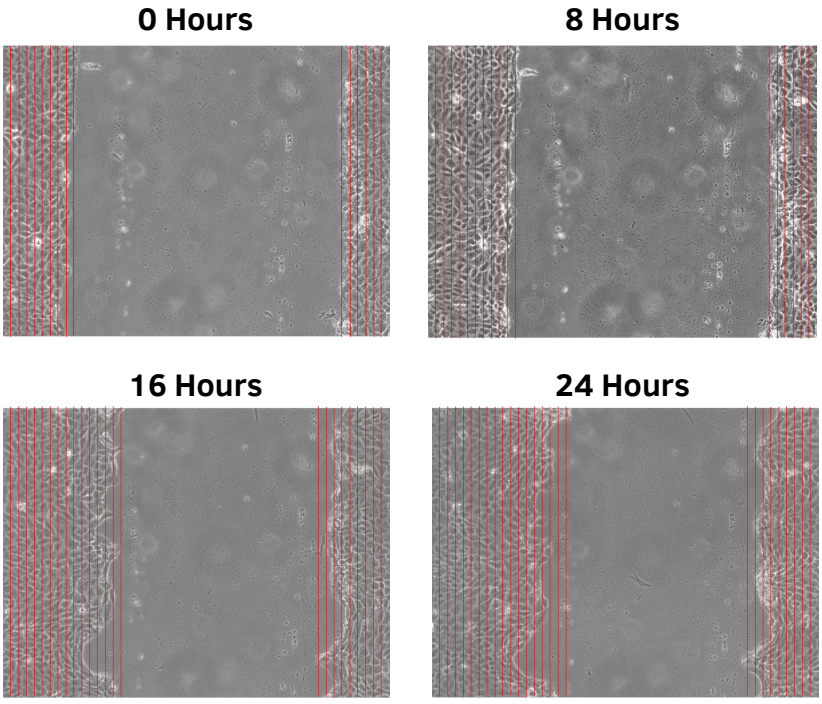

Figure 2. Microscopy images.

The following images show the traces and posterior distributions of the parameters of interest, which were obtained by implementing JAGS using two chains, 50000 iterations, a burning equal to 2000, and a thinning equal to 30.

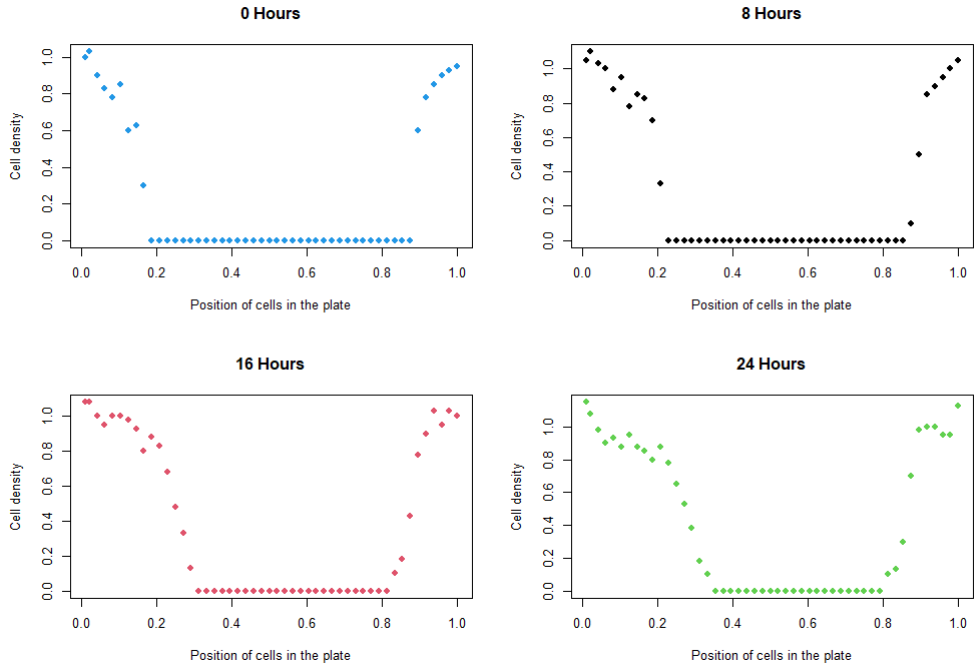

Figure 3. Data obtained. The x-axis represents the position of the cells in the dish, and the y-axis the cell density.

The following table shows the estimated values for a, b, α, and $\tau = \frac{1}{\sigma^2}$. For this Bayesian estimation we used the quadratic loss function, which turns out to be the posterior mean of $\boldsymbol{\theta}$. Then, the estimator of θ, denoted by θ^*, is obtained as the mean of the parameter values of the MCMC output.

Table 1. Parameter estimation.

Parameter	θ^*	Deviation	$\widehat{R}$
a	0.046	0.031	1.003
b	1.315	0.713	1.002
α	0.641	0.148	1.001
τ	42.037	4.415	1.001

Note: $\widehat{R}$ is the potential scale reduction factor.

We observe that the estimated value for alpha is far from 1, and so that the solution of the model is very different for the ordinary derivative alpha equal to 1. Using the data in Table 1, we obtain the model fit as follows

$$D_t^{0.641} u = 0.046 u_{xx} + 1.315 u, \quad t = 0, 8, 16, 24, \quad 0 < x < 1,$$

$$u(x,0) = \begin{cases} 1, & 0 \le x \le 0.20, \\ 0, & 0.20 \le x \le 0.88, \\ 1, & 0.88 \le x \le 1. \end{cases}$$

6. Conclusions

A mathematical model based on a diffusion equation with fractional order was proposed to describe the migration of HaCat cells in an *in vitro* wound healing assay. Bayesian analysis theory allowed us to solve the related inverse problem, where the JAGS package, within the R software, was of great help in finding samples of the posterior distributions and thus we were able to estimate the parameters of the model. In this work, both the direct and inverse problems were considered for a Fisher-type diffusion equation where a solution for the direct problem was given via the Fourier method and, by applying Bayesian theory, we solved the inverse problem; that is, the traces and estimated posterior distributions of the parameters were obtained through experimental data, as can be seen in the Figure 4. This helped to satisfactorily describe the behavior of cell density from the data obtained in the wound closure migration assay, as shown in Figure 5.

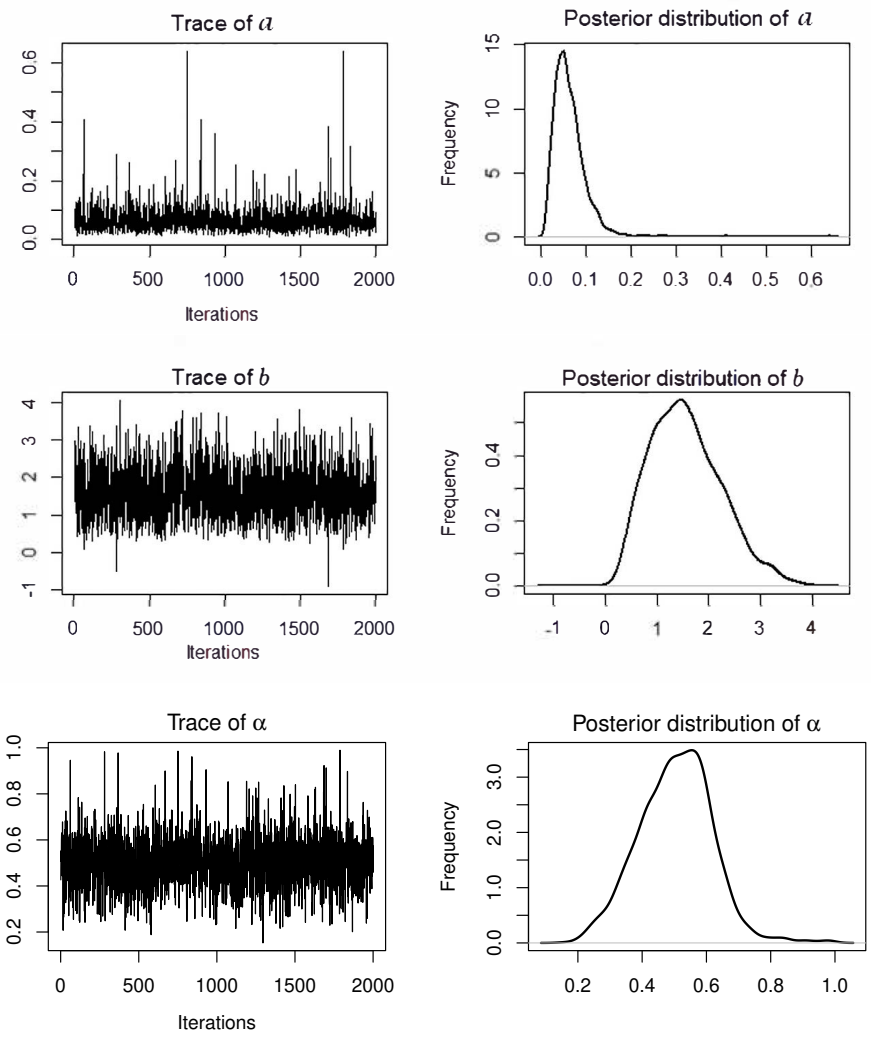

Figure 4. Trace and density functions of the estimated parameters a, b, and α. We observe that the distribution of the trace retains a stationary value and has a constant variance, which indicates good convergence.

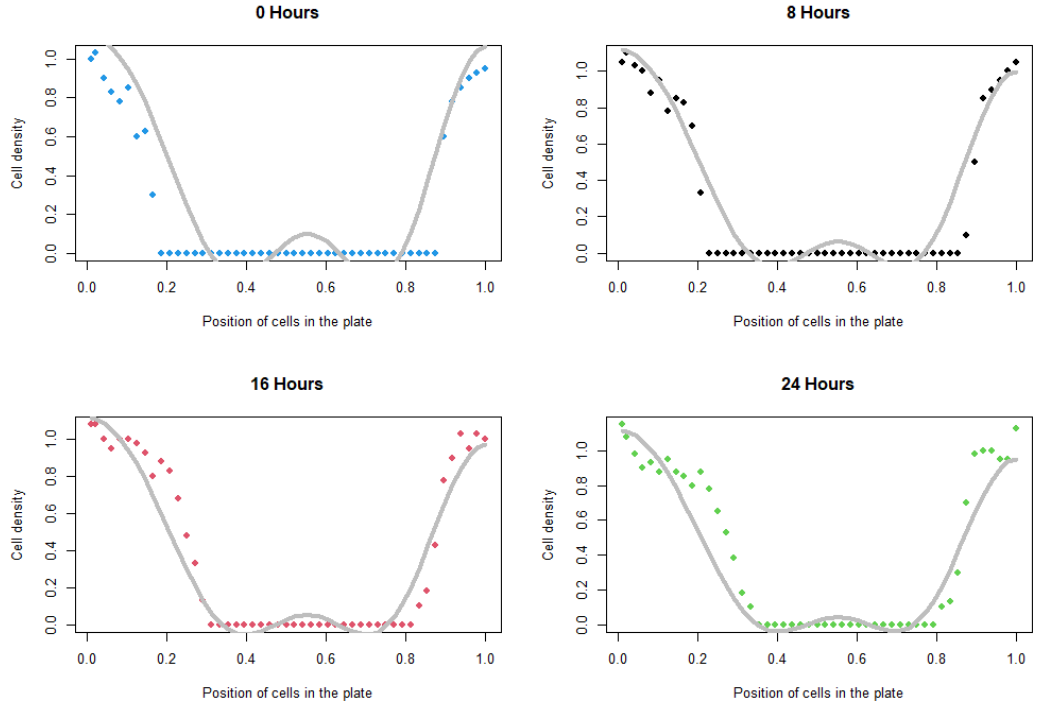

Figure 5. The lines represent the fitted model of (3.1), and the points are the cell density observations of the wound closure assay.

Use of AI tools declaration

The authors declare they have not used Artificial Intelligence (AI) tools in the creation of this article.

Acknowledgments

The authors gratefully acknowledge the financial support of the Postgraduate Study Fellowship by CONAHCYT, Mexico, (grant number: 1079596).

Conflict of interest

The authors declare there is no conflict of interest.

References

1. R. McLennan, L. Dyson, K. W. Prather, J. A. Morrison, R. E. Baker, P. K. Maini, et al., Multiscale mechanisms of cell migration during development: Theory and experiment, *Development*, **139** (2012), 2935–2944. http://doi.org/10.1242/dev.081471
2. J. A. Sherratt, P. Martin, J. D. Murray, J. Lewis, Mathematical models of wound healing in embryonic and adult epidermis, *Math. Med. Biol.: J. IMA*, **9** (1992), 175–196. https://doi.org/10.1093/imammb/9.3.177

3. P. Friedl, D. Gilmour, Collective cell migration in morphogenesis, regeneration and cancer, *Nat. Rev. Mol. Cell Biol.*, **10** (2009), 445–457. https://doi.org/10.1038/nrm2720
4. L. Oswald, S. Grosser, D. M. Smith, J. A. Käs, Jamming transitions in cancer, *J. Phys. D: Appl. Phys.*, **50** (2017), 483001. http://doi.org/10.1088/1361-6463/aa8e83
5. A. R. A. Anderson, A hybrid mathematical model of solid tumour invasion: The importance of cell adhesion, *Math. Med. Biol.: J. IMA*, **22** (2005), 163–186. http://doi.org/10.1093/imammb/dqi005
6. J. Zahm, H. Kaplan, A. Hérard, F. Doriot, D. Pierrot, P. Somelette, et al., Cell migration and proliferation during the in vitro wound repair of the respiratory epithelium, *Cytoskeleton*, **37** (1997), 33–43.
7. A. Tremel, A. Cai, N. Tirtaatmadja, B. D. Hughes, G. W. Stevens, K. A. Landman, et al., Cell migration and proliferation during monolayer formation and wound healing, *Chem. Eng. Sci.*, **64** (2009), 247–253. https://doi.org/10.1016/j.ces.2008.10.008
8. M. C. Robson, D. P. Hill, M. E. Woodske, D. L. Steed, Wound healing trajectories as predictors of effectiveness of therapeutic agents, *Arch. Surg.*, **135** (2000), 773–777. http://doi.org/10.1001/archsurg.135.7.773
9. J. A. Sherratt, J. D. Murray, Models of epidermal wound healing, *Proc. R. Soc. B.*, **241** (1990), 29–36. https://doi.org/10.1098/rspb.1990.0061
10. P. K Maini, D. L. S. McElwain, D. I. Leavesley, Traveling wave model to interpret a wound-healing cell migration assay for human peritoneal mesothelial cells, *Tissue Eng.*, **10** (2004), 475–482. http://doi.org/10.1089/107632704323061834
11. D. P. Stonko, L. Manning, M. Starz-Gaiano, B. E. Peercy, A mathematical model of collective cell migration in a three-dimensional, heterogeneous environment, *PloS one*, **10** (2015), 0122799. https://doi.org/10.1371/journal.pone.0122799
12. L. Chen, K. Painter, C. Surulescu, A. Zhigun, Mathematical models for cell migration: A non-local perspective. *Philos. Trans. R. Soc., B.*, **375** (2020), 20190379. https://doi.org/10.1098/rstb.2019.0379
13. B. Bonilla, M. Rivero, L. Rodríguez-Germá, J. J. Trujillo, Fractional differential equations as alternative models to nonlinear differential equations, *Appl. Math. Comput.*, **187** (2007), 79–88. https://doi.org/10.1016/j.amc.2006.08.105
14. F. J. Ariza-Hernandez, J. Sanchez-Ortiz, M. P. Arciga-Alejandre, L. X. Vivas-Cruz, Bayesian analysis for a fractional population growth model, *J. Appl. Math.*, **2017** (2017), 9654506. https://doi.org/10.1155/2017/9654506
15. M. Du, Z. Wang, H. Hu, Measuring memory with the order of fractional derivative, *Sci. Rep.*, **3** (2013), 3431. https://doi.org/10.1038/srep03431
16. S. L. Zeger, M. R. Krim, Generalized linear models with random effects; a Gibbs sampling approach, *J. Am. Stat. Assoc.*, **86** (1991), 79–86. http://doi.org/10.1080/01621459.1991.10475006
17. S. Chib, E. Greenberg, Understanding the metropolis-hastings algorithm, *Am. Stat.*, **49** (1995), 327–335. https://doi.org/10.2307/2684568
18. The R Foundation, The R Project for Statistical Computing, 2024. Available from: https://www.r-project.org/.

19. S. Sturtz, U. Ligges, A. Gelman, R2WinBUGS: A package for running WinBUGS from R, *J. Stat. Software*, **12** (2005), 1–16. http://doi.org/10.18637/jss.v012.i03

20. Y. Su, M. Yajima, Package 'R2jags', 2024. Available from: https://cran.r-project.org/web/packages/R2jags/R2jags.pdf.

21. M. Plummer, JAGS: A program for analysis of Bayesian graphical models using Gibbs sampling, in *Proceedings of the 3rd International Workshop on Distributed Statistical Computing*, (2003), 1–10.

22. R. M. Neal, Slice sampling, *Ann. Statist.*, **31** (2003), 705–767. http://doi.org/10.1214/aos/1056562461

AIMS Press